Search for Non-Trivial Band Topology in Double-Exchange Models

Aditya Vyas

A dissertation submitted for the partial fulfilment of BS-MS dual degree in Science

Indian Institute of Science Education and Research Mohali
April 2017

Certificate of Examination

This is to certify that the dissertation titled **Search for Non-Trivial Band Topology in Double-Exchange Models** submitted by **Aditya Vyas** (Reg. No. MS12016) for the partial fulfillment of BS-MS dual degree programme of the Institute, has been examined by the thesis committee duly appointed by the Institute. The committee finds the work done by the candidate satisfactory and recommends that the report be accepted.

Dr. Abhishek Chaudhuri Dr. Yogesh Singh Dr. Sanjeev Kumar
(Supervisor)

Dated: April 21, 2017

Declaration

The work presented in this dissertation has been carried out by me under the guidance of Dr. Sanjeev Kumar at the Indian Institute of Science Education and Research Mohali.

This work has not been submitted in part or in full for a degree, a diploma, or a fellowship to any other university or institute. Whenever contributions of others are involved, every effort is made to indicate this clearly, with due acknowledgement of collaborative research and discussions. This thesis is a bonafide record of original work done by me and all sources listed within have been detailed in the bibliography.

Aditya Vyas
(Candidate)

Dated: April 21, 2017

In my capacity as the supervisor of the candidates project work, I certify that the above statements by the candidate are true to the best of my knowledge.

Dr. Sanjeev Kumar
(Supervisor)

Acknowledgement

Before I get into all the things, I would like to add a few words of appreciation for the people who have helped me throughout my thesis work right from its beginning.

This work required a lot of guidance and support, and I owe my deepest gratitude to my supervisor, Dr. Sanjeev Kumar for all the invaluable discussions, his constant encouragement and his devotion to me. Under his guidance, I came to know about so many new aspects and new methods to solve for the energy dispersions of different types of systems. He brought me into the position of understanding some of the fundamental concepts of topological insulators and edge states. He has been very supportive throughout my thesis work. I also want to thank Dr. Abhishek Chaudhuri for his constant motivation.

I am also thankful to my colleagues Sanjib Kumar Das and Abhinay Vardhan who gave me various ideas to code the problem and helped me in plotting graphs using different software. I would also like to thank my parents and friends for their unconditional support during this thesis work.

Aditya Vyas

List of Figures

List of Tables

Contents

Abstract

As a new kind of state of the materials, topological insulators have been intensively studied by researchers very recently. The name is a little confusing. It does not have anything to do with the shape or with some abstract topology, and the interesting feature is not the insulating. The main feature of topological insulators is that they carry current along the surface but do not conduct current through the bulk of the material. We know the electrons spin in a quantum mechanical manner and encounter random collisions with other atoms and electrons, and produce magnetic field but spinning electrons on the surface of a topological insulator are protected from disruption by any quantum effects that's why we call them topologically protected. This exciting feature can make materials beneficial for spin related electronics, which would use the orientation of the electron spin to encode information. Topological Insulators bring a great opportunity to expand our understanding of solid state physics. Their applicability could also span the area of quantum computation. In my thesis work, I would try to deliver the basic understanding of these materials and their behavior with the help of some models. I would try to search for the non-trivial topology in double-exchange models via interaction of conduction electrons with localized moments. I would also like to extend this work ahead as there is so much to discover in this area and also it is the most interesting field for researchers in the condensed matter physics.

Chapter 1

Introduction

1.1 Overview

We see different types of materials around us. The difference is characterised in terms of qualitatively different physical properties. For example, based on the electrical transport properties we can classify materials as metals, insulators, semi-conductors and superconductors. The band theory of electrons[Kit66] was one of the greatest discovery of quantum mechanics in the 1920s which could successfully describe all aforementioned behaviors except superconductivity. In a band insulator, completely filled bands are separated by an energy gap from completely empty bands, the gap represents the energy cost to mobilize electrons. In contrast, materials with partially filled bands are conductors.

The discovery of the Quantum Hall Effect (1980)[KDP80] has proved that we can not just divide materials into band insulators and metals, not even within the simple band theory. In the quantum Hall effect, a strong magnetic field confines the motion of electrons in the bulk, but the same field forces them into delocalized exotic metallic states on the surface. These surface states are topologically protected which means that electrons travelling on such surfaces are insensitive to scattering by impurities and imperfections. It turns out that the QH state is just one example of a class of electronic states which are known as topological insulators.

1.2 Topological Insulators

Topological insulators are materials that are insulating in the bulk but have conducting edge or surface states which means they can conduct electricity on the surface. This conducting surface is a direct consequence of the nontrivial topology. When we experimentally study an insulating sample, inside our sample the system is an insulator, and outside the sample, the air or vacuum (depending on the experimental environment) is also an insulator. So we are in fact dealing with two insulators: the sample and the environment. If the quantum wavefunction of the sample shares the same topology as the environment, we call it a conventional insulator. Most of insulators that we know belong to this family, e.g. glass, rubber, plastic, the air and vacuum. In addition to these conventional insulators, there also exist some other insulators whose quantum wavefunctions are topologically different from the environment (say vacuum). If this is the case, we call the material a topological insulator.

A topological insulator typically has a conducting surface (although not always). One way to understand the existence of such a conducting surface is to consider a path with one end inside the sample and the other end outside. Because the topology of the quantum wavefunction inside is different from outside, somewhere along this path (usually at the surface of the sample), the quantum wavefunction shall change its topology. However, topology is not something that can be changed adiabatically. For example, we cannot deform a cylinder into a Mobius stripe. The only way to achieve this objective is to destroy the cylinder first (cut it) and then glue it back into a Mobius stripe[ians]. For insulators, if we want to change the topology of the quantum wavefunction, the same needs to be done. We have to destroy the insulator first, just as we cut the cylinder. What do we mean by destroying an insulator? Well, we know that if something is not an insulator, it is probably a conductor. In other words, when we destroy a insulator, we shall expect a conductor. Coming back to a topological insulator, when we move from inside the sample to outside, the topology changes at the interface. We also know that when topology is changed, the insulator needs to be destroyed, which results in a conductor. If we combine all the information together, it tells us that at the surface of the sample, where topology changes, a conductive layer shall arise.

Topological insulators are made possible because of two main features of quantum mechanics:

- **Time-reversal symmetry** means the physics is independent of the direction of the flow of time. For example, we record a video of any physical process and run it backward and if all the events shown in the backward running movie are allowed by the lows of physics or we are not able to determine just by watching the video if the video is being played in the forward direction or the backward direction, then this process is following the "time-reversal symmetry".

- **Spin-orbit interaction** means an interaction of a particle's spin with its motion. For example, we take an electron. As the electron orbits around the nucleus, it creates a magnetic field $\vec{B}$. This electron also has an intrinsic property called the electron spin and it also creates a spin magnetic dipole moment μ_s. Now this means that the spin magnetic dipole moment μ_s will feel a torque due to the magnetic field $\vec{B}$ created by the orbit of the electron. This interaction between the orbital angular momentum and the electron spin angular momentum is known as the "spin-orbit interaction".

If we talk about a non-interacting topological insulator, then the electronic band structure of the bulk looks just like an ordinary band insulator in which the Fermi level falls between the conduction and valence bands, but on the surface of a topological insulator there are special states that continuously connect bulk conduction and valance bands, as shown in figure 1.1 .

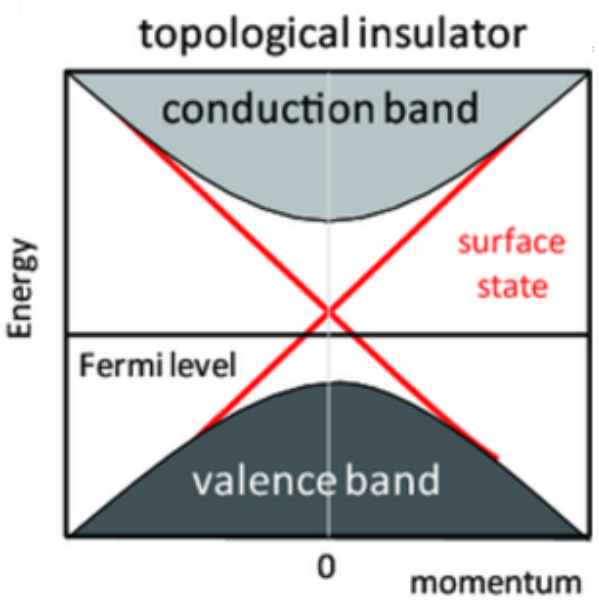

Figure 1.1: Band structure for a topological insulator.[Sch14]

1.3 Topology

Topology is a major area of mathematics that studies the properties of the objects that are preserved under smooth deformations. For example a coffee cup transforming into a doughnut are topologically equivalent as illustrated in figure 1.2. The idea

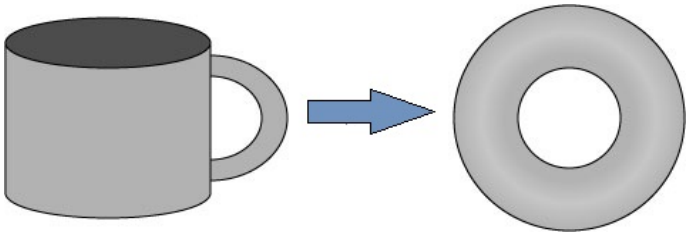

Figure 1.2: A continuous deformation of a coffee cup into a doughnut.

of topology comes from geometry. If two objects can not be transformed into each other via adiabatic deformations (such as stretching, crumpling and bending, but not tearing or gluing), then we say that they have different topology.

The topological invariant is a quantity that does not change under smooth deformation. The Gauss-Bonnet theorem[Gri13] states that the integral of the curvature over the whole surface is a topological invariant. We can give the similar argument for solid state systems like the integer quantum hall effect and topological insulators. In these systems the Brillouin zone plays the role of the surface and the Berry phase plays the role of the curvature.

1.4 Fundamental Concepts

The theory of topological band insulators can be perfectly described using the concept of adiabatic phases. I would like to define some of the basic concepts: the Berry phase, the Berry curvature and the Chern number using the language of discrete quantum states. This gives an efficient method for calculating Chern number, which is a very important topological invariant in the context of 2D electron systems.

1. Berry phase

For defining Berry phase we first need to calculate the relative phase of two non-orthogonal quantum states ψ_1 and ψ_2, which can be written as

$$\gamma_{12} = -arg\langle\psi_1|\psi_2\rangle \tag{1.1}$$

where $arg(z) \in (-\pi, \pi]$ and denotes the phase of the complex number z. The relative phase γ_{12} also satisfies

$$e^{-i\gamma_{12}} = \frac{\langle\psi_1|\psi_2\rangle}{|\langle\psi_1|\psi_2\rangle|} \tag{1.2}$$

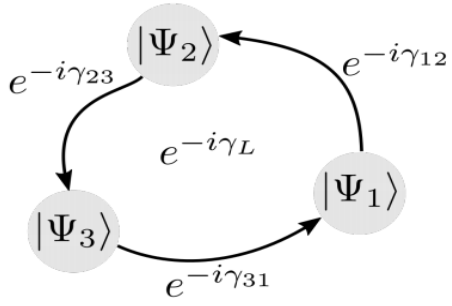

Figure 1.3: The Berry phase γ_L for the loop of three quantum states.[AOP16]

Now we are in position to define Berry phase. We take N quantum states $|\psi_j\rangle$, with j = 1,2,3,...,N, and order them in a loop. For ordered list L=(1,2,...,N), we can define the Berry phase as

$$\gamma_L = -arg e^{-i(\gamma_{12}+\gamma_{23}+...+\gamma_{N1})} = -arg(\langle\psi_1|\psi_2\rangle\langle\psi_2|\psi_3\rangle.....\langle\psi_N|\psi_1\rangle) \tag{1.3}$$

2. Berry flux

In the similar manner, we write the Berry phase γ_L for a finite 2D rectangular lattice with sites labelled by $n, m \in \mathbb{Z}$,$1 \leq n \leq N$ and $1 \leq m \leq M$, as

$$\gamma_L = -arg\ exp\left[-i\left(\sum_{n=1}^{N-1}\gamma_{(n,1),(n+1,1)} + \sum_{m=1}^{M-1}\gamma_{(N,m),(N,m+1)} + \sum_{n=1}^{N-1}\gamma_{(n+1,M),(n,M)} + \sum_{m=1}^{M-1}\gamma_{(1,m+1),(1,m)}\right)\right] \tag{1.4}$$

For simplifying the above calculation, we define Berry flux F_{nm} for each of the plaquette on the grid as

$$F_{nm} = -arg\ exp\left[-i\left(\gamma_{(n,m),(n+1,m)} + \gamma_{(n+1,m),(n+1,m+1)} + \gamma_{(n+1,m+1),(n,m+1)} + \gamma_{(n,m+1),(n,m)}\right)\right] \tag{1.5}$$

where n,m indicate the lower left corner of the plaquette. Now we can directly get the Berry phase by first multiplying all the plaquette phase factors and then taking negative argument of the term.

$$\prod_{n=1}^{N-1}\prod_{m=1}^{M-1} e^{-iF_{nm}} = exp\left[-i\sum_{n=1}^{N-1}\sum_{m=1}^{M-1} F_{nm}\right] \tag{1.6}$$

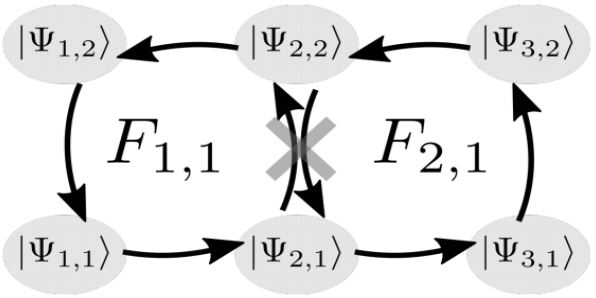

Figure 1.4: The Berry phase γ_L defined on a lattice as the sum of the Berry fluxes $F_{1,1}$ and $F_{2,1}$.[AOP16]

We see that each internal edge is being shared between two plaquettes and the contribution from both the plaquettes will be complex conjugate of each other and when we will multiply the phase factors, it will give us unity. The Berry phase can be written as

$$\gamma_L = -arg\ exp\left[-i\sum_{n=1}^{N-1}\sum_{m=1}^{M-1} F_{nm}\right] \tag{1.7}$$

3. Berry curvature

We can express the gauge invariant Berry phase as a surface integral of a gauge invariant quantity. This quantity is the Berry curvature. In a discrete case, the Berry curvature can be evaluated from the Berry phase around one small plaquette divided by the area of that plaquette.

4. Chern number

The Chern number is an intrinsic property of the band structure and has various effects on the transport properties of the system. Let us take the periodic boundary conditions and map the square lattice grid on the surface of a torus. where n+1 is written as (n mod N)+1 and m+1 is written as (m mod M)+1. Periodic boundary

condition states that if we write the product of the Berry flux phase factors of all the plaquettes then it will give us 1.

$$\prod_{n=1}^{N}\prod_{m=1}^{M} e^{-iF_{nm}} = 1 \tag{1.8}$$

We can define the Chern number Q associated to our structure as

$$Q = \frac{1}{2\pi}\sum_{nm} F_{nm} \tag{1.9}$$

1.5 Thesis Plan

I would like to introduce the work done by me. I first derive the understanding of the topological insulators from some elementary models in which it is rather simple to see the topological effects arising just from constraining the systems to some finite size. These topological effects are able to govern some of the great theories of physics. I start my discussion with the bulk and then plot dispersion relations for the finite size lattices and see that as soon as we constrain our system, we start seeing the edge states connecting the two bands which were earlier separated by some finite band gap. These interesting phenomenons can also be seen in some other systems where the total spin of electrons in other orbitals are together producing the localized magnetic moment at every lattice site. I explore the understanding of these non-trivial effects in cubic lattices with some unusual magnetic structures. For that, I first derive the double-exchange model starting from ferromagnetic Kondo lattice model. This model has its limitations. It forces the electron spin to align in the direction of the localized spin that means we are only interested in low energy region. I use the double-exchange model for calculating energy dispersion relations for lattices with qualitatively different localized moments configurations. We know that topologically non-trivial band structures are characterized by non-zero Chern numbers and edge states and my task is to check the possibility of creating such band structures via interaction of conduction electrons with localized moments.

I will arrange the content of this thesis as follows. In chapter 2, I will introduce and discuss two elementary models describing non-trivial band topology. These are the SSH model and the Kane-Mele model. Then in chapter 3, I will discuss the double-exchange model, calculate the dispersion relations for different spin configurations and I will try to check the non triviality of some of the band structures.

Chapter 2

Elementary Models for Topological Insulators

2.1 The Su-Schrieffer-Heeger (SSH) model

The SSH model is the simplest one dimensional model which helps us in understanding the basic concepts of topological insulators. It describes spinless fermions hopping on a one-dimensional lattice with staggered hopping amplitudes.

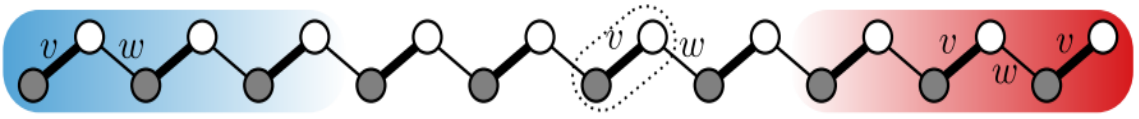

Figure 2.1: Geometry of the SSH model.[AOP16]

Here in the above figure a 1D chain of polyacetylene with two atoms in the unit cell is shown. Every lattice site in the chain is hosting a single state. Filled (empty) circles are sites on sublattice A (B). The hopping amplitudes are different for different bonds. v (thick lines) denotes the intracell hopping amplitude and w (thin lines) denotes the intercell hopping amplitude. The left and right edge regions are indicated as blue and red backgrounds respectively. The m = 6th cell is circled by a dotted line.

2.1.1 The SSH Hamiltonian

We take a chain consist of N units cells. The practical choice of unit cells includes two sites per unit cell, one on sublattice A, and one on sublattice B. We assume the total number of sites (M) to be even, M = 2N. We denote the site index as m, where

m = 1,2,.....,N and sublattice index as j, where j = A, B. Now the SSH Hamiltonian can be written as:

$$\hat{H} = v \sum_{m=1}^{N} \left(|m, B\rangle \langle m, A| + h.c. \right) + w \sum_{m=1}^{N-1} \left(|m+1, A\rangle \langle m, B| + h.c. \right) \tag{2.1}$$

Here $|m, A\rangle$ and $|m, B\rangle$ are the states of the chain where the electron is in unit cell m, in the site on sublattice A and B respectively. There are some underlying assumptions in writing the above Hamiltonian :

- We are neglecting the interactions between the electrons.
- The spin degree of freedom is completely absent from the SSH model.
- For simplicity, the hopping amplitudes v and w are taken to be real non-negative i.e. v,$w \geq 0$.

2.1.2 Bulk Hamiltonian

Any real solid-state system has two parts, a bulk and a boundary. Bulk is the most important part of a solid. It determines almost all the physical properties associated with the given solid. In the thermodynamic limit of $N \to \infty$, the physics in the bulk does not depend upon the boundaries of the system. By taking the periodic boundary conditions the bulk Hamiltonian is defined as :

$$\hat{H}_{bulk} = \sum_{m=1}^{N} \left(v \; c^{\dagger}_{m,A} c_{m,B} + w \; c^{\dagger}_{(m \; mod \; N)+1,A} c_{m,B} \right) + h.c. \tag{2.2}$$

Now in order to extract the dispersion relation $E(k)$ for the bulk, we first Fourier transform the above Hamiltonian using following transformations:

$$c_{m,j} = \frac{1}{\sqrt{N}} \sum_{k} e^{i\vec{k}\cdot\vec{R_m}} c_{k,j} \tag{2.3}$$

$$c^{\dagger}{}_{m,j} = \frac{1}{\sqrt{N}} \sum_{k} e^{-i\vec{k}\cdot\vec{R_m}} c^{\dagger}{}_{k,j} \tag{2.4}$$

we calculate the bulk momentum space Hamiltonian:

$$\begin{aligned}\hat{H}_{bulk}(k) = \sum_{m=1}^{N} \Bigg[v \left(\frac{1}{\sqrt{N}} \sum_{k} e^{-i\vec{k}\cdot\vec{R_m}} {c^{\dagger}}_{k,A} \right) \left(\frac{1}{\sqrt{N}} \sum_{k'} e^{i\vec{k'}\cdot\vec{R_m}} c_{k',B} \right) \\ + w \left(\frac{1}{\sqrt{N}} \sum_{k} e^{-i\vec{k}\cdot(\vec{R_m}+\hat{i})} {c^{\dagger}}_{k,A} \right) \left(\frac{1}{\sqrt{N}} \sum_{k'} e^{i\vec{k'}\cdot\vec{R_m}} c_{k',B} \right) \Bigg] + h.c.\end{aligned} \tag{2.5}$$

$$\begin{aligned}\hat{H}_{bulk}(k) = v \sum_{k} \sum_{k'} \left(\frac{1}{N} \sum_{m=1}^{N} e^{i(\vec{k'}-\vec{k})\cdot\vec{R_m}} \right) {c^{\dagger}}_{k,A} c_{k',B} + h.c \\ + w \sum_{k} \sum_{k'} \left(\frac{1}{N} \sum_{m=1}^{N} e^{i(\vec{k'}-\vec{k})\cdot\vec{R_m}} \right) e^{-ik_x} {c^{\dagger}}_{k,A} c_{k',B} + h.c\end{aligned} \tag{2.6}$$

where $\frac{1}{N}\sum_{m=1}^{N} e^{i(\vec{k'}-\vec{k})\cdot\vec{R_m}} = \delta_{k,k'}$ is a Kronecker delta function. We can denote k_x as just k because we are only constraining our lattice in 1D. The bulk momentum space Hamiltonian can be written as :

$$\hat{H}_{bulk}(k) = \sum_{k} \left(v + we^{-ik}\right) {c^{\dagger}}_{k,A} c_{k,B} + \left(v + we^{+ik}\right) {c^{\dagger}}_{k,B} c_{k,A} \tag{2.7}$$

We write the above Hamiltonian in matrix form as :

$$\hat{H}_{bulk}(k) = \sum_{k} \begin{bmatrix} c^{\dagger}_{k,A} & c^{\dagger}_{k,B} \end{bmatrix} \begin{bmatrix} 0 & v + we^{-ik} \\ v + we^{+ik} & 0 \end{bmatrix} \begin{bmatrix} c_{k,A} \\ c_{k,B} \end{bmatrix} \tag{2.8}$$

where the bulk momentum space Hamiltonian matrix

$$H(k) = \begin{bmatrix} 0 & v + we^{-ik} \\ v + we^{+ik} & 0 \end{bmatrix} \tag{2.9}$$

Now by diagonalising the above Hamiltonian matrix, we get the simplest form of the energy dispersion relation $E(k)$ as :

$$E(k) = \pm\sqrt{v^2 + w^2 + 2vw\ cos(k)} \tag{2.10}$$

The bulk momentum space Hamiltonian matrix $H(k)$ of any two band system which means a system with two non-equivalent sites, is also defined as

$$H(k) = d_0(k)\hat{\sigma}_0 + d_x(k)\hat{\sigma}_x + d_y(k)\hat{\sigma}_y + d_z(k)\hat{\sigma}_z = d_0(k)\hat{\sigma}_0 + \mathbf{d}(k)\hat{\sigma} \tag{2.11}$$

Using Eqs. 2.9 and 2.11, we find out the components of **d**-vector for SSH model, where $d_0(k) = 0$ and $d_x, d_y, d_z \in \mathbb{R}$.

$$d_x(k) = v + w\cos(k) \qquad d_y(k) = w\sin(k) \qquad d_z(k) = 0 \tag{2.12}$$

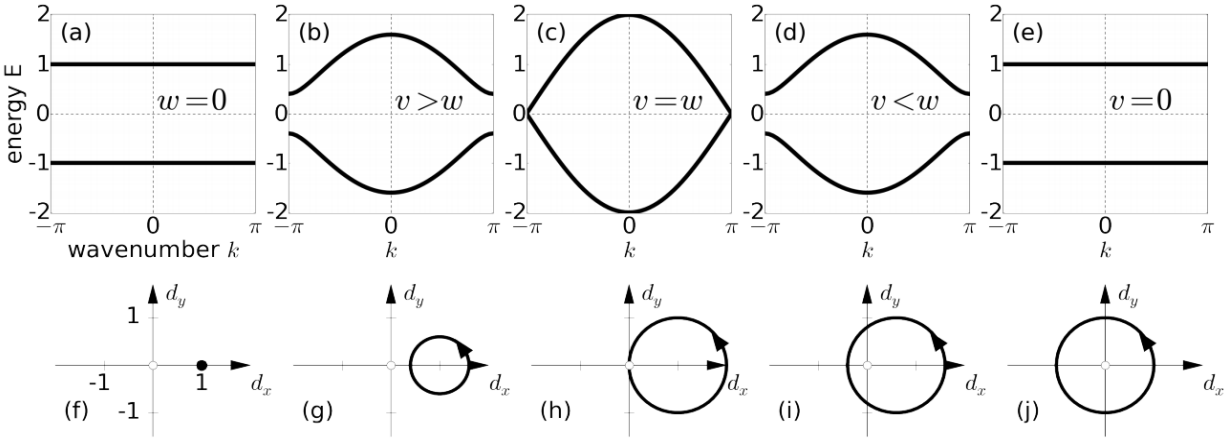

Figure 2.2: Dispersion relations of the SSH model for five choices of the parameters and corresponding plots of the path of the tip of the vector d(k).[AOP16]

There are some properties of the **d**-vector.

- If we take some general two-band insulators then the path traced out by the **d**-vector should not necessarily be a circle, but it has to be a closed loop because of the periodicity of the Hamiltonian.
- For describing an insulator, this path needs to avoid the origin.
- The topology of this loop can be determined by *bulk winding number* $'\nu'$ which is also a very good topological invariant and counts the number of times the loop winds around the origin.

Winding number of the SSH model

By the definition of the bulk winding number we can clearly see that for the SSH model, when we change the value of parameter w by fixing the value of parameter v as 1, winding number ν also changes from 0 to 1 and it is undefined when $v = w$. It means whenever winding number changes from 0 to 1, the band gap closes and reopens and we say that it is going from trivial phase to the topological phase. Why do we say so? It can be clearly understood from the next section.

2.1.3 Edge States

Any material can be seen as two parts; one the bulk part and other the boundary. The bulk part plays a very important role in characterizing most of the properties of the material. The boundary part of any material determines the topological behavior of the material. We will try to see the edge state behavior for SSH model first with the fully dimerized limit and then we will take a definite real space lattice for understanding the edge states business.

Fully dimerized limits

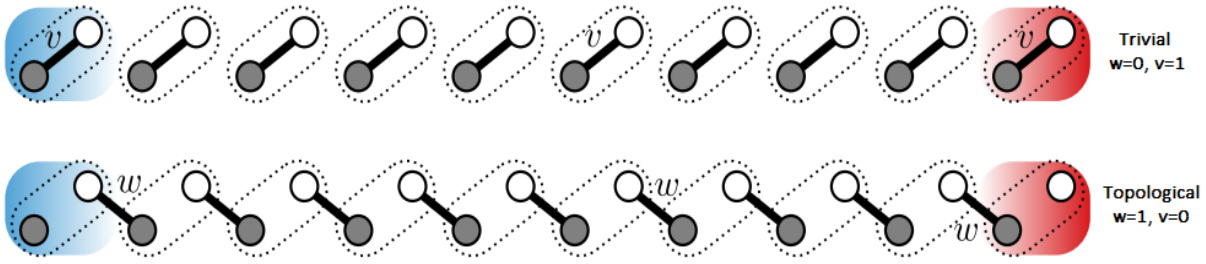

Figure 2.3: Fully dimerized limits of the SSH model.[AOP16]

- In the trivial case (v=1, w=0) where the bulk Hamiltonian is $\hat{H}(k) = \hat{\sigma}_x$, we have

$$\hat{H}\left(|m, A\rangle \pm \langle m, B|\right) = \pm\left(|m, A\rangle \pm \langle m, B|\right) \tag{2.13}$$

  It gives all energy eigenstates of the SSH chain with energy eigenvalues ± 1.

- In the topological case (v=0, w=1) where the bulk Hamiltonian is $\hat{H}(k) = \hat{\sigma}_x cos(k) + \hat{\sigma}_y sin(k)$, we have

$$\hat{H}\left(|m, B\rangle \pm \langle m+1, A|\right) = \pm\left(|m, B\rangle \pm \langle m+1, A|\right) \tag{2.14}$$

  It has more energy eigenstates than those listed in Eq.2.14. Each end of the chain hosts a single eigenstate at zero energy. These are called edge states.

$$\hat{H}\,|1, A\rangle = \hat{H}\,|N, B\rangle = 0 \tag{2.15}$$

Extending the fully dimerized limit

By extending we mean that now we are no more in fully dimerized limit. We turn on the intracell hopping amplitude ν, increase it from 0 to 3 by fixing w = 1 and try to plot the energy spectra for a finite-sized lattice of N = 10 unit cells. First we write Hamiltonian for the given lattice using Eq.2.1. We simplify the Hamiltonian and write it in the matrix form in terms of parameters v and w. We fix the value of w as 1 and calculate the eigenvalues of the Hamiltonian for each value of parameter v by changing it from 0 to 3. There will be 20 eigenvalues for each value of parameter v. Now we plot those 20 eigenvalues for each value of parameter v and get the energy spectrum as

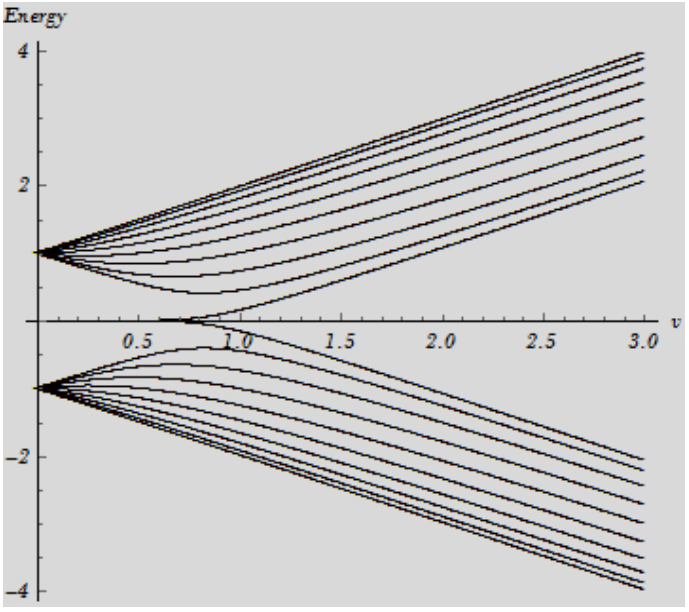

Figure 2.4: Energy spectrum of a finite-sized SSH model consisting of N = 10 unit cells.

2.2 Kane-Mele model

A valid description of the edge states can be clearly noticed from the Kane-Mele model, which describes electrons on the 2D honeycomb lattice.

2.2.1 Hamiltonian

The Kane-Mele Hamiltonian consists of two terms. The first term is the usual nearest neighbor hopping term and the second term is the spin-orbit coupling which connects every site(i) with the next nearest neighbor site(j) with the spin dependent amplitude ν_{ij}, where $\nu_{ij} = -\nu_{ji} = \pm 1$. Which value does ν_{ij} take, depends upon the orientation of the two nearest neighbor bonds. If electron goes to the nearest neighbor site and take right(left) turn to go to the next site then ν_{ij} will be -1(1). By introducing second neighbor tight binding model, the Kane-Mele Hamiltonian[KM05] can be written as

$$H = \sum_{\langle ij\rangle\alpha} t c^{\dagger}_{i\alpha} c_{j\alpha} + \sum_{\langle\langle ij\rangle\rangle\alpha\beta} i t_2 \nu_{ij} s^{z}_{\alpha\beta} c^{\dagger}_{i\alpha} c_{j\beta} \tag{2.16}$$

where α and β denote two spins; spin up and spin down at two sites i and j. There are four combinations of spins possible at two sites ($\uparrow\uparrow, \uparrow\downarrow, \downarrow\uparrow, \downarrow\downarrow$). $s^{z}_{\alpha\beta}$ is a Pauli z spin matrix;

$$S_z = \frac{\hbar}{2}\begin{bmatrix} 1 & 0 \\ 0 & -1 \end{bmatrix} \tag{2.17}$$

2.2.2 Bulk Dispersion Relation Derivation

We plot the bulk dispersion relation using the above Hamiltonian. We have two sublattices A and B in one unit cell. We define two primitive vectors $\vec{a_1}$ and $\vec{a_2}$ for our lattice as

$$\vec{a_1} = a\left(\frac{\sqrt{3}}{2}\hat{i} + \frac{3}{2}\hat{j}\right), \vec{a_2} = a\left(-\frac{\sqrt{3}}{2}\hat{i} + \frac{3}{2}\hat{j}\right) \tag{2.18}$$

where a denotes the distance between two lattice points.

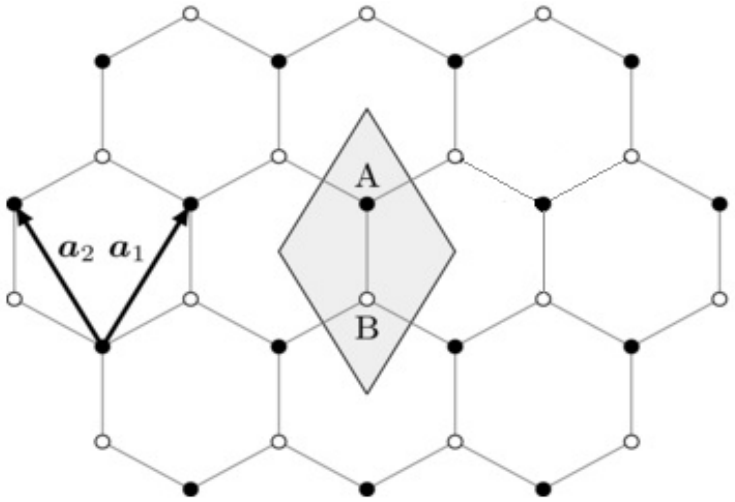

Figure 2.5: Geometry of the 2D honeycomb lattice with primitive lattice vectors $\vec{a_1}$ and $\vec{a_2}$. Shaded area is representing the unit cell with sublattices A and B.[EJT12]

We first break the Hamiltonian in two parts.

$$H = H(1) + H(2) \tag{2.19}$$

We write first and second term of the Hamiltonian in the real space basis as

$$\begin{aligned} H(1) = t \sum_{\langle ij \rangle} \Big[\Big(& c^\dagger_{iA\uparrow} c_{iB\uparrow} + c^\dagger_{iA\uparrow} c_{(i+\vec{a_1})B\uparrow} + c^\dagger_{iA\uparrow} c_{(i+\vec{a_2})B\uparrow} + h.c. \Big) \\ & + \Big(c^\dagger_{iA\downarrow} c_{iB\downarrow} + c^\dagger_{iA\downarrow} c_{(i+\vec{a_1})B\downarrow} + c^\dagger_{iA\downarrow} c_{(i+\vec{a_2})B\downarrow} + h.c. \Big) \Big] \end{aligned} \tag{2.20}$$

$$\begin{aligned} H(2) = \sum_{\langle\langle ij \rangle\rangle} \Big[& \Big(it_2 (c^\dagger_{iA\uparrow} c_{(i+\vec{a_1})A\uparrow} - c^\dagger_{iA\uparrow} c_{(i+\vec{a_2})A\uparrow} - c^\dagger_{iA\uparrow} c_{(i+\vec{a_1}-\vec{a_2})A\uparrow}) + h.c. \Big) \\ & + \Big(it_2 (-c^\dagger_{iA\downarrow} c_{(i+\vec{a_1})A\downarrow} + c^\dagger_{iA\downarrow} c_{(i+\vec{a_2})A\downarrow} + c^\dagger_{iA\downarrow} c_{(i+\vec{a_1}-\vec{a_2})A\downarrow}) + h.c. \Big) \\ & + \Big(it_2 (-c^\dagger_{iB\uparrow} c_{(i+\vec{a_1})B\uparrow} + c^\dagger_{iB\uparrow} c_{(i+\vec{a_2})B\uparrow} + c^\dagger_{iB\uparrow} c_{(i+\vec{a_1}-\vec{a_2})B\uparrow}) + h.c. \Big) \\ & + \Big(it_2 (c^\dagger_{iB\downarrow} c_{(i+\vec{a_1})B\downarrow} - c^\dagger_{iB\downarrow} c_{(i+\vec{a_2})B\downarrow} - c^\dagger_{iB\downarrow} c_{(i+\vec{a_1}-\vec{a_2})B\downarrow}) + h.c. \Big) \Big] \end{aligned} \tag{2.21}$$

Now after doing Fourier transformation of the above Hamiltonian, we get

$$H = \sum_k \left[L \left(c^\dagger_{A\uparrow} c_{A\uparrow} - c^\dagger_{A\downarrow} c_{A\downarrow} - c^\dagger_{B\uparrow} c_{B\uparrow} + c^\dagger_{B\downarrow} c_{B\downarrow} \right) + M c^\dagger_{A\uparrow} c_{B\uparrow} + N c^\dagger_{B\uparrow} c_{A\uparrow} \right] \quad (2.22)$$

where;

$$L = -2t_2 \sin\left(\frac{\sqrt{3}k_x a}{2}\right)\left(\cos\left(\frac{3k_y a}{2}\right) - \cos\left(\frac{\sqrt{3}k_x a}{2}\right)\right) \quad (2.23)$$

$$M = t\left(1 + 2e^{i\frac{3k_y a}{2}}\cos\left(\frac{\sqrt{3}k_x a}{2}\right)\right) \quad (2.24)$$

$$N = t\left(1 + 2e^{-i\frac{3k_y a}{2}}\cos\left(\frac{\sqrt{3}k_x a}{2}\right)\right) \quad (2.25)$$

We can write the above Hamiltonian in the matrix form as

$$H = \begin{bmatrix} c^\dagger_{A\uparrow} & c^\dagger_{B\uparrow} & c^\dagger_{A\downarrow} & c^\dagger_{B\downarrow} \end{bmatrix} \begin{bmatrix} L & M & 0 & 0 \\ N & -L & 0 & 0 \\ 0 & 0 & -L & M \\ 0 & 0 & N & L \end{bmatrix} \begin{bmatrix} c_{A\uparrow} \\ c_{B\uparrow} \\ c_{A\downarrow} \\ c_{B\downarrow} \end{bmatrix} \quad (2.26)$$

In order to get the dispersion relation, we need to diagonalize the Hamiltonian matrix H(k). We can see that the Hamiltonian is in the block diagonal form and we can clearly notice that both the blocks will give the same eigenvalues. So we just diagonalize only one block to get the eigenvalues λ.

$$\begin{vmatrix} L-\lambda & M \\ N & -L-\lambda \end{vmatrix} = 0 \quad (2.27)$$

Using Eqs.2.23, 2.24 and 2.25, we can calculate the eigenvalues;

$$\lambda^2 = L^2 + NM \quad (2.28)$$

After solving the above equation, we get

$$\begin{aligned} E^2(k) &= \lambda^2 \\ &= \Big(3 + 2\cos(2X) + 4\cos(X)\cos(Y\sqrt{3})\Big) + \\ &\quad 4{t_2}^2\sin^2(x)\Big(\cos^2(Y\sqrt{3}) + \cos^2(X) - 2\cos(X)\cos(Y\sqrt{3})\Big) \end{aligned} \tag{2.29}$$

where;

$$X = \frac{k_x a\sqrt{3}}{2} \quad , \quad Y = \frac{k_y a\sqrt{3}}{2} \tag{2.30}$$

We now fix the parameters as t = 1 and $t_2 = 0.03$ and plot the dispersion relation E(k) using Eq.2.29.

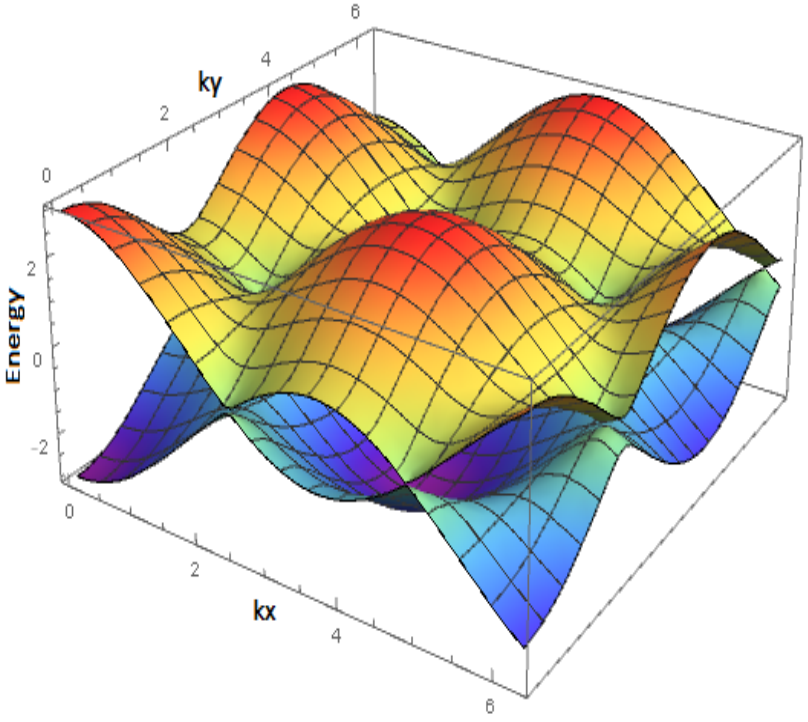

Figure 2.6: Dispersion relation for the bulk Hamiltonian.

We see that there is a gap between the two bands. We also plot the dispersion relation for t_2=0 and we claim that it should show the same dispersion as we see for graphene when we just take the nearest neighbor hopping term.

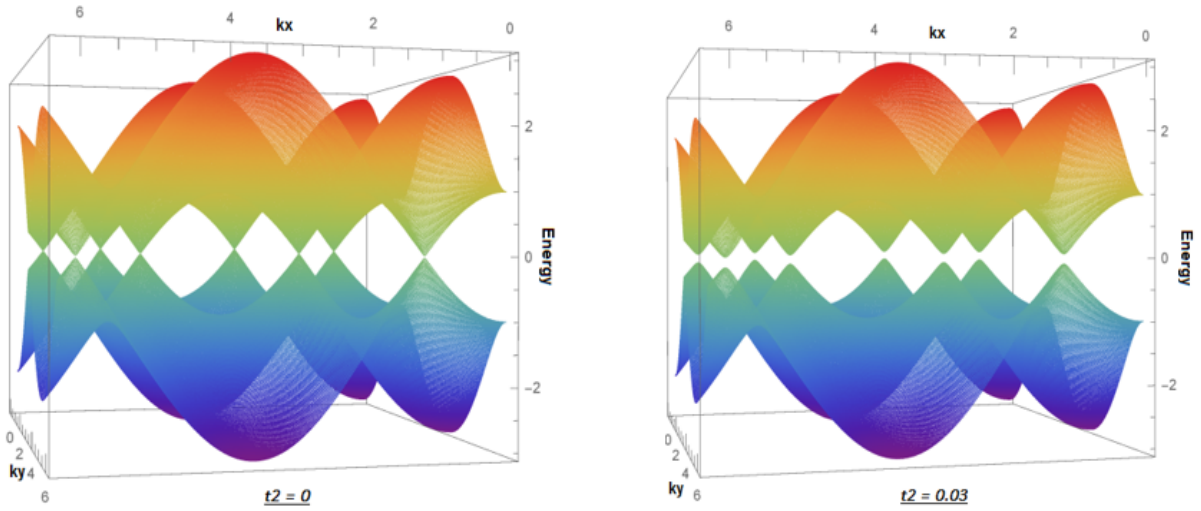

Figure 2.7: Bulk dispersion relation for different value of parameters t_2.

We know that the Hamiltonian of any two-band system can be written in terms of **d**-vector and Pauli matrices. We try to calculate the same **d**-vector for Kane-Mele model as we did for SSH model and we get,

$$d_x = t\left(1 + 2\cos\left(\frac{3k_y a}{2}\right)\cos\left(\frac{k_x a\sqrt{3}}{2}\right)\right) \tag{2.31}$$

$$d_y = -2t\sin\left(\frac{3k_y a}{2}\right)\cos\left(\frac{k_x a\sqrt{3}}{2}\right) \tag{2.32}$$

$$d_z = -4t_2\sin\left(\frac{k_x a\sqrt{3}}{2}\right)\left[\cos\left(\frac{3k_y a}{2}\right) - \cos\left(\frac{k_x a\sqrt{3}}{2}\right)\right] \tag{2.33}$$

2.2.3 Edge States

For our discussion we take a strip of graphene with three hexagonal rings in y direction(12 atoms) and periodic boundary in x direction. We take unit cell as shown in figure 2.8. We first write the Hamiltonian in real space and then Fourier transform it in terms of k_x because we have periodic boundary condition only in x-direction so for this case k_x will be a good quantum number. In the Kane-Mele Hamiltonian, we are also taking into account the spin degree of freedom. We write the Hamiltonian for

both the spins of electrons and then in order to get the energy dispersion relation we solve for the eigenvalues of 24×24 matrix because there are 12 sites in one unit cell and each can have either up or down electron. Then we plot one-dimensional energy bands for a strip of graphene modeled by Kane-Mele Hamiltonian, taking t=1 and $t_2 = 0.1$.

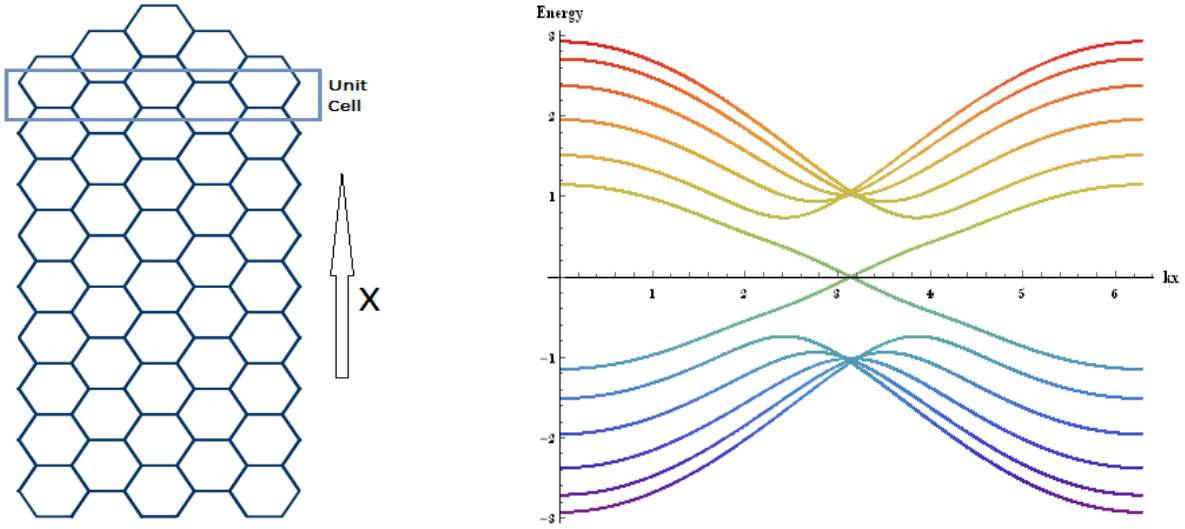

Figure 2.8: A strip of graphene consisting of 12 atoms in one unit cell in y-direction and one dimensional energy bands for the same, showing spin filtered edge states.

We see that in a strip of graphene the edges are along the zigzag direction in the graphene plane. When we solve for the bulk Hamiltonian, we get the dispersion relation with a gap between the two bands but as we constrain our system, we see two states connecting the two bands. These are called the "edge states". These edge states are spin filtered which means that electrons with opposite spin propagate in opposite directions and the conduction only occurs on the edges.

Chapter 3

Double-Exchange Model

3.1 Introduction

Double exchange was first introduced in 1951 by Zener. He wanted to describe ferromagnetism in the manganese oxide perovskites. He considered Mn oxide compounds which contain both Mn^{+3} and Mn^{+4}. He proposed that these materials have some kind of close connection between ferromagnetism and conduction. He gives a brief explanation by saying that e_g electrons on Mn^{+3} ions could hop to vacant e_g orbitals available on neighboring Mn^{+4} ions. Mn^{+3} contains four 3d electrons in its outer shell and in the perovskites, when the 3d band splits, three of the electrons occupy the lower three-fold degenerate localized t_{2g} orbitals, one electron goes in an upper two-fold degenerate delocalized e_g orbital. We know that whenever electron hops from one site to another, it preserves its spin and the Hund's rule coupling also plays a very important role since it favors an alignment of the e_g spin with that of the localized t_{2g} electrons. When e_g electron hops from Mn^{+3} to Mn^{+4}, it forces all the t_{2g} electrons on Mn^{+4} to align in the same direction as itself. This hopping is not a direct hopping between the atoms, O^{-2} works as an intermediate ion. This ferromagnetic alignment induced by the hopping is called "double-exchange interaction".

3.2 Hamiltonian

There are two degrees of freedom; one is conduction electrons and another is localized spins. It says that electrons are coupled to the localized spins defined at the same lattice sites. The spin of the electrons is constrained to be parallel to that of the localized spins. As a consequence, this restriction modulate the electron hopping

amplitude between lattice sites and it only depends on the relative orientation of the core spins. The double-exchange Hamiltonian[ACF$^+$01] can be written as

$$H_{DE} = -\sum_{ij}\Big(t_{ij}c_i^\dagger c_j + h.c.\Big) + J_{AF}\sum_{ij}\mathbf{S}_i\cdot\mathbf{S}_j \tag{3.1}$$

where J_{AF} is the strength of the antiferromagnetic coupling between the localized spins, which is considered to be vanishingly small and t_{ij} can be written as:

$$t_{ij} = t\Big\langle\theta_i\phi_i|\theta_j\phi_j\Big\rangle \tag{3.2}$$

where;

$$\Big\langle\theta_i\phi_i|\theta_j\phi_j\Big\rangle = \cos(\frac{\theta_i}{2})\cos(\frac{\theta_j}{2}) + \sin(\frac{\theta_i}{2})\sin(\frac{\theta_j}{2})e^{-i(\phi_i-\phi_j)} \tag{3.3}$$

3.3 Derivation

The double-exchange Hamiltonian can be derived from the model which describes a lattice of atoms with strong intra-atomic Hunds coupling ($J<0$ and $|J|\gg t$) between electrons in different orbitals. The simplest Hamiltonian[Gul04] which includes this effect is that of the ferromagnetic Kondo lattice,

$$H_{FK} = -t\sum_{i,j,\sigma}(c_{i,\sigma}^\dagger c_{j,\sigma} + h.c.) + J\sum_i S_{ic}\cdot S_i \tag{3.4}$$

Here S_i denotes the localized spin and S_{ic} is the electronic spin operator defined as $(S_{ic})_\alpha = \sum_{\sigma\sigma'} c_{i,\sigma}^\dagger(\sigma_\alpha)_{\sigma\sigma'}c_{i,\sigma'}$ where $\sigma_\alpha(\alpha$=x,y,z) are the Pauli matrices.

Now we apply canonical transformation on the above Hamiltonian. It preserves the form of the Hamilton's equation but it might not preserve the Hamiltonian itself. We write down the Hamiltonian in new basis where the spin quantization axis is different for different sites and it always points along the direction of the localized spin. We introduce polar and azimuthal angles θ and ϕ respectively and define our

transformation[KvdBK10] as

$$\begin{aligned}\begin{bmatrix} c_{i\uparrow} \\ c_{i\downarrow} \end{bmatrix} &= \begin{pmatrix} \cos(\frac{\theta_i}{2})e^{\frac{i\phi_i}{2}} & -\sin(\frac{\theta_i}{2})e^{\frac{i\phi_i}{2}} \\ \sin(\frac{\theta_i}{2})e^{-\frac{i\phi_i}{2}} & \cos(\frac{\theta_i}{2})e^{-\frac{i\phi_i}{2}} \end{pmatrix} \begin{bmatrix} d_{ip} \\ d_{ia} \end{bmatrix} \\ &\equiv M(\theta_i, \phi_i) \begin{bmatrix} d_{ip} \\ d_{ia} \end{bmatrix}\end{aligned} \tag{3.5}$$

Here $d_{ip}(d_{ia})$ annihilates an electron at site i with spin parallel(anti-parallel) to the core spin. In terms of d operators the first term of the above Hamiltonian reads:

$$H = -\sum_{\langle ij\rangle\sigma}\sum_{s,s'} t(f_{ss'}d^{\dagger}_{is}d_{js'} + h.c.) \tag{3.6}$$

The coefficients $f_{ss'}$ are explicitly given by,

$$\mathbf{T} = \begin{bmatrix} f_{pp} & f_{pa} \\ f_{ap} & f_{aa} \end{bmatrix} = M^{\dagger}(\theta_i, \phi_i) \cdot M(\theta_j, \phi_j) \tag{3.7}$$

$$\mathbf{T} = \begin{pmatrix} \cos(\frac{\theta_i}{2})e^{-\frac{i\phi_i}{2}} & \sin(\frac{\theta_i}{2})e^{\frac{i\phi_i}{2}} \\ -\sin(\frac{\theta_i}{2})e^{-\frac{i\phi_i}{2}} & \cos(\frac{\theta_i}{2})e^{\frac{i\phi_i}{2}} \end{pmatrix} \begin{pmatrix} \cos(\frac{\theta_j}{2})e^{\frac{i\phi_j}{2}} & -\sin(\frac{\theta_j}{2})e^{\frac{i\phi_j}{2}} \\ \sin(\frac{\theta_j}{2})e^{-\frac{i\phi_j}{2}} & \cos(\frac{\theta_j}{2})e^{-\frac{i\phi_j}{2}} \end{pmatrix} \tag{3.8}$$

Now we can compare the Eqs.3.7 and 3.8 and find out the expressions for the coefficients $f_{ss'}$.

$$f_{pp} = \cos(\frac{\theta_i}{2})\cos(\frac{\theta_j}{2})e^{-\frac{i(\phi_i-\phi_j)}{2}} + \sin(\frac{\theta_i}{2})\sin(\frac{\theta_j}{2})e^{\frac{i(\phi_i-\phi_j)}{2}} \tag{3.9}$$

$$f_{pa} = \sin(\frac{\theta_i}{2})\cos(\frac{\theta_j}{2})e^{\frac{i(\phi_i-\phi_j)}{2}} - \cos(\frac{\theta_i}{2})\sin(\frac{\theta_j}{2})e^{-\frac{i(\phi_i-\phi_j)}{2}} \tag{3.10}$$

$$f_{ap} = \cos(\frac{\theta_i}{2})\sin(\frac{\theta_j}{2})e^{\frac{i(\phi_i-\phi_j)}{2}} - \sin(\frac{\theta_i}{2})\cos(\frac{\theta_j}{2})e^{-\frac{i(\phi_i-\phi_j)}{2}} \tag{3.11}$$

$$f_{aa} = \sin(\frac{\theta_i}{2})\sin(\frac{\theta_j}{2})e^{-\frac{i(\phi_i-\phi_j)}{2}} + \cos(\frac{\theta_i}{2})\cos(\frac{\theta_j}{2})e^{\frac{i(\phi_i-\phi_j)}{2}} \tag{3.12}$$

For strong intra-atomic Hund's rule coupling $|J| \gg t$, we can retain the low energy behavior by constraining electron spin to be parallel to the localized spin. It means we just consider f_{pp} term for writing the Hamiltonian. The final Hamiltonian will be:

$$H = -\sum_{\langle ij \rangle} t(f_{pp} d^{\dagger}_{ip} d_{jp} + h.c.) \tag{3.13}$$

We see that the above Hamiltonian which we derived by taking the first term of the ferromagnetic Kondo lattice model is exactly same as the first term of the double-exchange Hamiltonian(Eq. 3.1) only when we take strong Hund's coupling.

3.4 Application of Double-Exchange Model

The double-exchange model describes noninteracting itinerant electrons moving on a lattice of static background spins whose moments are typically large compared to that of the electron spins, and hence may be treated classically. We use the double-exchange model for calculating dispersion relations for cubic lattices with qualitatively different spin configurations. In particular we focus on noncoplaner configurations.

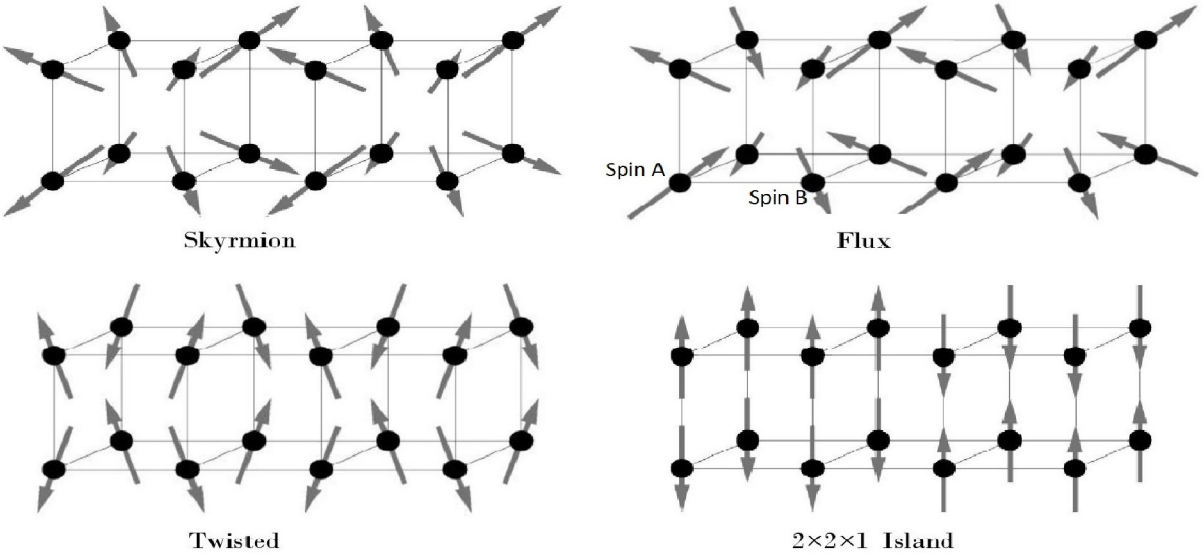

Figure 3.1: Unusual Magnetic Structures.[ACF+01]

3.4.1 Flux Phase

It consists of 8 localized spins on eight lattice sites of the unit cube. Four of them are pointing towards the center of the cube and another four are pointing out of the center as shown in figure 3.1. Spin direction for flux phase is denoted as

$$\left(\frac{(-1)^{y+z}}{\sqrt{3}}, \frac{(-1)^{x+z}}{\sqrt{3}}, \frac{(-1)^{x+y}}{\sqrt{3}}\right) \tag{3.14}$$

Derivation of dispersion relation

We first calculate the value of hopping amplitude t_{ij} as defined in the double-exchange model, for all the eight lattice sites of the unit cube. We get only two different values of t_{ij} such that if four of them are giving $(t_{ij})_A$ then the other four are giving $(t_{ij})_B$. We conclude that there are only two nonequivalent sites A and B. Each of them has a localized spin pointing in different directions and their interactions with the neighbouring atoms will also be different. We take a unit cell with two sites in which 'A' is at one site and 'B' is at another site, We see that these unit cells are arranged in a triangular lattice if we arrange them in two dimensional space and the same 2d sheet of unit cells repeat in z direction. Now we define three primitive vectors for arranging the unit cells in 3D space. Those primitive vectors are given as

$$\vec{a_1} = a\left(\hat{i} + \hat{j}\right), \vec{a_2} = a\left(-\hat{i} + \hat{j}\right), \vec{a_3} = a\hat{k} \tag{3.15}$$

Here 'a' is the distance between two lattice points. For simplicity, we will take a=1. Following table shows components of the hopping amplitude t_{ij} in every direction for two nonequivalent sites A and B.

Spin Interactions		
Components	Spin A	Spin B
$(t_{ij})_x$	$(1-i)/\sqrt{6}$	$(1+i)/\sqrt{6}$
$(t_{ij})_y$	$(1+i)/\sqrt{6}$	$(1-i)/\sqrt{6}$
$(t_{ij})_z$	$1/\sqrt{3}$	$-(1/\sqrt{3})$

Table 3.1: Spin interactions between the neighbours in every direction.

The double-exchange Hamiltonian for the nearest neighbour interactions can be written as:

$$H = -\sum_{ij} t_{ij} c_i^\dagger c_j + t_{ij}^* c_j^\dagger c_i \tag{3.16}$$

We write the full Hamiltonian in real space as

$$\begin{aligned} H = \sum_i & \frac{(1-i)}{\sqrt{6}} c_{iA}^\dagger c_{iB} + \frac{(1+i)}{\sqrt{6}} c_{iB}^\dagger c_{iA} + \frac{(1+i)}{\sqrt{6}} c_{iA}^\dagger c_{(i+\vec{a_2})B} \\ & + \frac{(1-i)}{\sqrt{6}} c_{(i+\vec{a_2})B}^\dagger c_{iA} + \frac{(1-i)}{\sqrt{6}} c_{iA}^\dagger c_{(i+\vec{a_2}-\vec{a_1})B} \\ & + \frac{(1+i)}{\sqrt{6}} c_{(i+\vec{a_2}-\vec{a_1})B}^\dagger c_{iA} + \frac{(1+i)}{\sqrt{6}} c_{iA}^\dagger c_{(i-\vec{a_1})B} + \frac{(1-i)}{\sqrt{6}} c_{(i-\vec{a_1})B}^\dagger c_{iA} \\ & + \frac{1}{\sqrt{3}} \left(c_{iA}^\dagger c_{(i+\vec{a_3})A} + c_{(i+\vec{a_3})A}^\dagger c_{iA} \right) - \frac{1}{\sqrt{3}} \left(c_{iB}^\dagger c_{(i+\vec{a_3})B} + c_{(i+\vec{a_3})B}^\dagger c_{iB} \right) \end{aligned} \tag{3.17}$$

Now in order to extract the dispersion relation $\epsilon(k)$, we Fourier transform the Hamiltonian H using the following transformations;

$$c_{iA}^\dagger = \frac{1}{\sqrt{N}} \sum_k e^{-i\vec{k}\cdot\vec{r_i}} c_{kA}^\dagger \tag{3.18}$$

$$c_{iA} = \frac{1}{\sqrt{N}} \sum_k e^{i\vec{k}\cdot\vec{r_i}} c_{kA} \tag{3.19}$$

After doing Fourier transformation of the above Hamiltonian, we get

$$\begin{aligned} H = \sum_k & e^{-ik_x} \left[2 \left(\frac{1-i}{\sqrt{6}} \right) \cos k_x + 2 \left(\frac{1+i}{\sqrt{6}} \right) \cos k_y \right] c_{kA}^\dagger c_{kB} \\ & + e^{ik_x} \left[2 \left(\frac{1-i}{\sqrt{6}} \right) \cos k_y + 2 \left(\frac{1+i}{\sqrt{6}} \right) \cos k_x \right] c_{kB}^\dagger c_{kA} \\ & + \left[\frac{2}{\sqrt{3}} \cos k_z \right] c_{kA}^\dagger c_{kA} - \left[\frac{2}{\sqrt{3}} \cos k_z \right] c_{kB}^\dagger c_{kB} \end{aligned} \tag{3.20}$$

Using the above Hamiltonian we can write the Hamiltonian matrix as

$$H(k) = \begin{bmatrix} \frac{2}{\sqrt{3}} \cos k_z & e^{-ik_x}\left(2\left(\frac{1-i}{\sqrt{6}}\right)\cos k_x + 2\left(\frac{1+i}{\sqrt{6}}\right)\cos k_y\right) \\ e^{ik_x}\left(2\left(\frac{1-i}{\sqrt{6}}\right)\cos k_y + 2\left(\frac{1+i}{\sqrt{6}}\right)\cos k_x\right) & -\frac{2}{\sqrt{3}}\cos k_z \end{bmatrix} \tag{3.21}$$

Now the main task is to diagonalize the matrix and get the dispersion relation. After digonalizing the above matrix, we get

$$\lambda^2 - \frac{4}{3}\cos^2(k_z) = \frac{4}{3}\cos^2(k_x) + \frac{4}{3}\cos^2(k_y) \tag{3.22}$$

$$\lambda = \epsilon(k) = \pm\sqrt{\frac{1}{3}\sum_{\mu=x,y,z}\cos^2 k_\mu} \tag{3.23}$$

Now we plot the dispersion relation for flux phase by fixing one parameter k_z to be constant. We plot dispersions for different values of k_z.

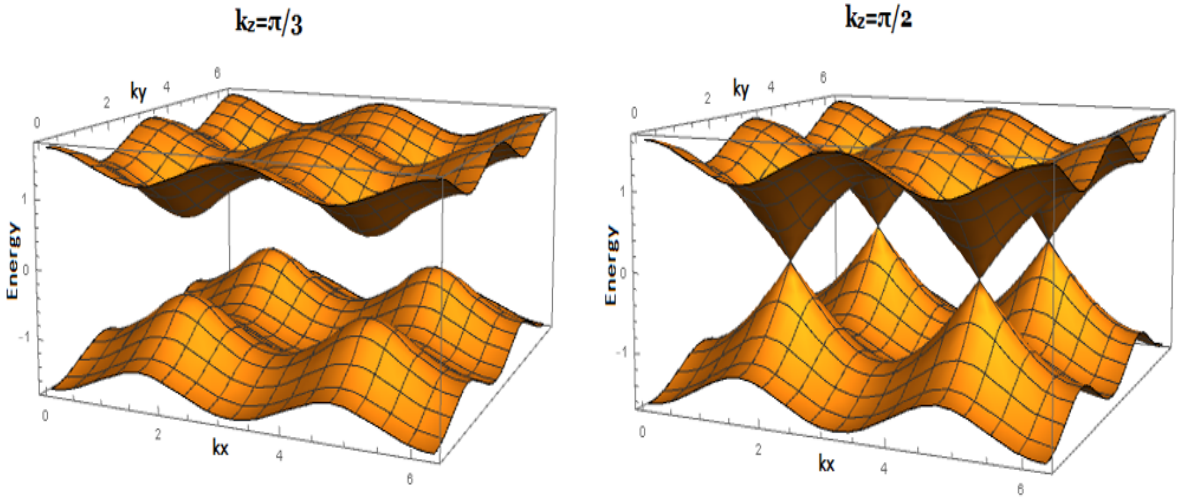

Figure 3.2: Dispersion relation for flux state.

We can follow the same approach for finding the dispersion relations for different spin configurations. Table 3.2 shows all the spin configurations and the dispersion relations of the different phases.

Table 3.2: Type of the phases, spin directions and electronic dispersion relations of the different phases are shown in the table[ACF$^+$01].The notation $[\cdot]$ stands for the integer part.

Type	**Spin Direction**	$\epsilon(\mathbf{k})/\mathbf{t}$
Ferromagnetic	$(0,0,1)$	$-2\sum_{\mu=1}^{3}\cos(k_\mu)$
A-AFM	$(0,0,(-1)^z)$	$-2\sum_{\mu=1}^{2}\cos(k_\mu)$
C-AFM	$(0,0,(-1)^{x+y})$	$-2\cos(k_3)$
G-AFM	$(0,0,(-1)^{x+y+z})$	0
Twisted	$(a(-1)^{x+y}, b(-1)^z, 0)$	$\pm 2[a^2\cos^2(k_3)+b^2(\cos(k_1)\pm\cos(k_2))^2]^{\frac{1}{2}}$
Flux	$\frac{((-1)^{y+z},(-1)^{x+z},(-1)^{x+y})}{\sqrt{3}}$	$\pm 2\left[\frac{1}{3}\sum_{\mu=1}^{3}\cos^2(k_\mu)\right]^{\frac{1}{2}}$
Skyrmion	$\frac{((-1)^{x},(-1)^{y},(-1)^{z})}{\sqrt{3}}$	$\pm 2\sqrt{\frac{2}{3}}\left[\sum_{\mu=1}^{3}\cos^2(k_\mu)\pm\sqrt{3\sum_{\mu\neq\nu}\cos^2(k_\mu)\cos^2(k_\nu)}\right]^{\frac{1}{2}}$
Helix	$(\cos(qz),\sin(qz),0)$	$-2\sum_{\mu=1}^{2}\cos(k_\mu)-2\cos(k_3+\frac{q}{2})\cos(\frac{q}{2})$
Island$(\frac{\pi}{2},\pi,\pi)$	$(0,0,(-1)^{[\frac{x}{2}]+y+z})$	-1,1
Island$(\frac{\pi}{3},\pi,\pi)$	$(0,0,(-1)^{[\frac{x}{3}]+y+z})$	$-\sqrt{2},0,\sqrt{2}$
Island$(\frac{\pi}{2},\frac{\pi}{2},\pi)$	$(0,0,(-1)^{[\frac{x}{2}]+[\frac{y}{2}]+z})$	-2,0,0,2

We will now be plotting the density of states for some of the above given dispersion relations. We can see the spread in energy i.e. the range of the energy available to be occupied by the electrons for each of the dispersion relation and we can compare this for all the phases.

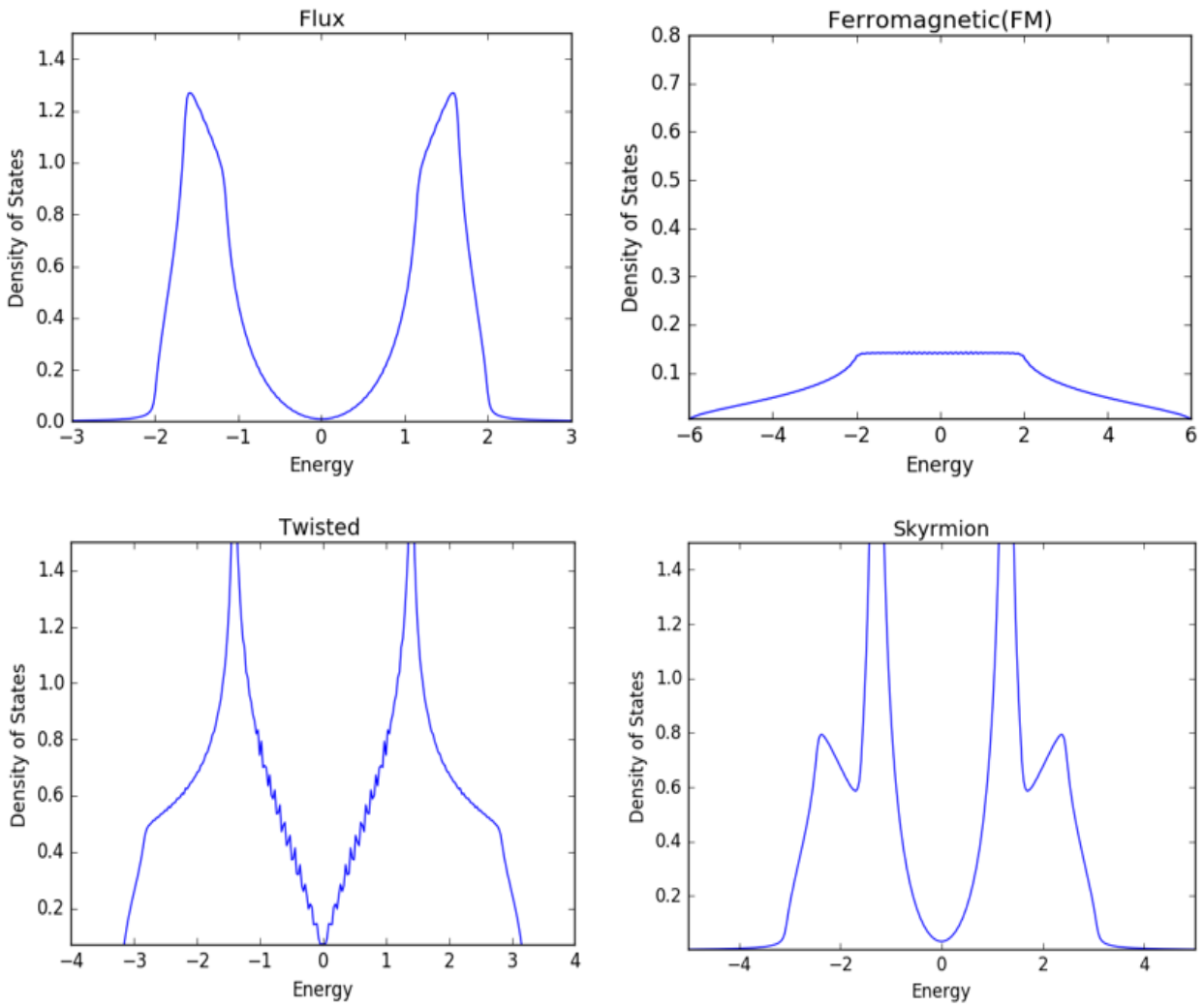

Figure 3.3: Density of states for several spin configurations by taking $100 \times 100 \times 100$ lattice.

3.5 Non-triviality of The Spin Configurations

For our discussion, by non-triviality we actually mean that for any magnetic textured system, if it is not possible to continuously transform it into conventional (topologically trivial) forms of spin order such as ferromagnetism or antiferromagnetism then it is called "non-trivial". Here in this section we would like to find out the non-trivial phases from the above mentioned spin configurations. For that, we will calculate topological charge for all the spin configurations and we know[Vit01](page 39) that if topological charge comes out to be 0 then it is trivial and if it is not zero then it is

non-trivial.

In order to locate the topological charges in the lattice model we follow the prescription of Berg and Lusher[BL81]. For each unit cube of the lattice we divide each of its six faces into two triangles. The particular division in triangles could give an uncertainty in the value of the topological charge. The three unit-normalized spins at the corners of a triangle I define a signed area A_I [CB01] on the unit sphere:

$$A_I = 2\tan^{-1}\frac{\vec{m}_i \cdot (\vec{m}_j \times \vec{m}_k)}{1 + \vec{m}_i \cdot \vec{m}_j + \vec{m}_i \cdot \vec{m}_k + \vec{m}_j \cdot \vec{m}_k} \tag{3.24}$$

where i, j, k form the triangle I and are ordered such that the surface vector points outward the unit cube. In terms of these areas the topological charge enclosed by the unit cube is given by

$$Q = \frac{1}{4\pi}\sum_{I=1}^{12} A_I \tag{3.25}$$

Now we calculate the topological charge(Q) for each of the above mentioned spin configurations and check if they are showing non-trivial behavior or not. We see that all the phases gives 0 value of the topological charge instead of one that is skyrmion phase. The value of topological charge for skyrmion phase is +1 as all the spins are pointing out from the center of the unit cube. If all the spins point towards the center then also it will show non-trivial behavior but the value of the topological charge in that case would be -1.

3.6 Conclusion

- We have seen the topological behaviors in both one dimension and two dimensions using the SSH model and the Kane-Mele model respectively, and we are able to produce the edge states plots for 1D and 2D lattices only if we use open boundary conditions. In case of periodic boundary conditions we get a band gap as we get for the bulk. We are also able to distinguish between the trivial and topological phases by just analysing the **d**-vector plot in one dimension but only when the z component of the **d**-vector is 0.

- We have used double-exchange model to describe different spin configurations like ferromagnetic, flux, helix, twisted, skyrmion etc. We have tried to check the non triviality for all the spin configurations and we have confirmed from the calculation of topological charges that the skyrmion phase is the only phase which shows the non-trivial topological behavior. The topological charge for the skyrmion phase was coming out to be +1 and it was 0 for all other spin configurations.

3.7 Future Outlook

- I would like to explore the SSH model by taking the next nearest neighbour hopping because this will give me the z-component of the **d**-vector, which was absent in the actual SSH model 2.12 and then I will try to see, how **d**-vector can be used to verify the topological behavior of the system like it does in SSH model.

- I would also like to see the direct relation of **d**-vector with the topological behavior of graphene from Kane-Mele model.

- I will also try to find out the similar **d**-vector technique for the four level systems so that we would be able to comment on the triviality or non-triviality of some band structures which has four bands in their dispersion relation like skyrmion and twisted phases as **d**-vector can only be written for two-band systems using Pauli matrices.

Bibliography

[ACF+01] JL Alonso, JA Capitán, LA Fernández, F Guinea, and Víctor Martín-Mayor, *Monte carlo determination of the phase diagram of the double-exchange model*, Physical Review B **64** (2001), no. 5, 054408.

[AOP16] János K Asbóth, László Oroszlány, and András Pályi, *A short course on topological insulators*, Lecture Notes in Physics **919** (2016).

[BL81] B Berg and Martin Lüscher, *Definition and statistical distributions of a topological number in the lattice o (3) σ-model*, Nuclear Physics B **190** (1981), no. 2, 412–424.

[CB01] MJ Calderón and L Brey, *Skyrmion strings contribution to the anomalous hall effect in double-exchange systems*, Physical Review B **63** (2001), no. 5, 054421.

[EJT12] Merab Eliashvili, George I Japaridze, and George Tsitsishvili, *The quantum group, harper equation and structure of bloch eigenstates on a honeycomb lattice*, Journal of Physics A: Mathematical and Theoretical **45** (2012), no. 39, 395305.

[Gri13] Pavel Grinfeld, *Introduction to tensor analysis and the calculus of moving surfaces*, Springer, 2013.

[Gul04] Miklós Gulácsi*, *The one-dimensional kondo lattice model at partial band filling*, Advances in physics **53** (2004), no. 7, 769–937.

[ians] Sun Group(Physics in a nut shell), *Topological states of matter*, http://www-personal.umich.edu.

[KDP80] K v Klitzing, Gerhard Dorda, and Michael Pepper, *New method for high-accuracy determination of the fine-structure constant based on quantized hall resistance*, Physical Review Letters **45** (1980), no. 6, 494.

[Kit66] Charles Kittel, *Introduction to solid state*, vol. 162, John Wiley & Sons, 1966.

[KM05] Charles L Kane and Eugene J Mele, *Quantum spin hall effect in graphene*, Physical review letters **95** (2005), no. 22, 226801.

[KvdBK10] Sanjeev Kumar, Jeroen van den Brink, and Arno P Kampf, *Spin-spiral states in undoped manganites: Role of finite hunds rule coupling*, Physical review letters **104** (2010), no. 1, 017201.

[Sch14] Scholarpedia, *Topological insulators*, www.scholarpedia.org/w/images/e/ed/TI˙fig2.

[Vit01] Giuseppe Vitiello, *My double unveiled: the dissipative quantum model of brain*, vol. 32, John Benjamins Publishing, 2001.